

Navigator Echo Collection for Sliding Interleaved Cylinder Acquisition

Kie Tae Kwon¹, Adam B Kerr¹, and Dwight G Nishimura¹

¹Stanford University, Stanford, CA, United States

Purpose: A sliding interleaved cylinder (SLINCYL) acquisition¹ has previously been incorporated into a steady-state free precession (SSFP) sequence to achieve improved artery-vein contrast in the lower extremities. In this work, we extended the sequence to collect navigator echoes without additional scan time to enable the use of a non-linear-phase RF excitation pulse.

Methods: SLINCYL: Similar to the original sliding interleaved k_y (SLINKY) acquisition², SLINCYL consists of a series of overlapped thin slabs (Fig. 1a, right). The slab location is incremented by a distance d equal to the resolution in the slab direction (z). For each slab, one of N_s partial sets of concentric cylinders³ is collected. This acquisition scheme enables the suppression of venetian blind artifacts by transforming inflow enhancement into k-space amplitude modulation². For the reconstruction, hybrid slices ($z-k_x-k_y$) are first generated from each slab after applying a 1D inverse Fourier transform in k_z . Then, each slice in z is formed independently by combining its relevant hybrid slices that are selected out of N_s consecutive slabs. In this step, k-space phase modulation across those hybrid slices needs to be corrected. For a linear-phase (LP) RF excitation pulse with a proper refocusing gradient, the modulation is mainly due to different transmit-frequency offsets of RF pulses for different slabs, which can be theoretically calculated and corrected⁴.

Navigator Echo for SSFP-based SLINCYL: To enable the correction of phase modulation even with a non-linear-phase RF pulse, a 1D navigator echo was collected ahead of the SSFP readout of each slab (Fig. 1b). The echo was acquired with a constant G_z gradient during the catalyzation cycles, which was exactly the same G_z gradient as that of each SSFP readout. Therefore, a 1D navigator echo in z can be collected while establishing the SSFP steady state during the catalyzation cycles.

Non-linear-phase (NLP) RF Pulse: An NLP pulse was designed by flipping the passband roots of the beta-polynomial of an LP SLR pulse^{5,6} (flip angle: 60°, duration: 1.2 ms, time-bandwidth: 8). The one with the minimum peak amplitude was chosen among those with less than 5% signal loss due to non-linear phase dispersion within each voxel in the passband. As a result, the peak amplitude was reduced to 0.145G (58% of the original pulse).

In Vivo Experiments: The calves of four healthy volunteers were scanned on a GE Excite 1.5 T scanner with the aforementioned NLP pulse and an LP pulse with the same peak amplitude (duration: 1.6 ms, time-bandwidth: 6). Imaging parameters of each thin slab of SLINCYL were: resolution = 1.2 mm isotropic, FOV = 340×340×38.4 mm³, TR = 6.2/6.6 ms (NLP/LP pulses), and 10 TRs of catalyzation cycles with cosine-ramp-weighted flip angles. 168 slabs ($N_s = 24$) were acquired to cover 17 cm in the S/I direction. Total scan time was around 3 min 20 s for both cases.

Results: Figure 2 shows targeted coronal maximum-intensity-projection (MIP) images of the calves of a subject for which phase modulation was corrected using either (a,c) theoretically calculated phase offsets based on the transmit-frequency offsets of RF pulses or (b,d) phase offsets extracted from 1D navigator echoes (Fig. 1c). For the LP pulse (a,b), the quality of the image is almost identical between those two correction methods. For the NLP pulse (c,d), only the correction using navigator echoes shows similar image quality to the LP-pulse cases.

Discussion/Conclusion: We demonstrated that the proposed scheme of navigator echo collection was feasible for SLINCYL, which allowed the use of an NLP RF excitation pulse that shortened TR and improved the slab profile compared to an LP RF pulse with the same peak amplitude. Unlike the original navigator scheme proposed with SLINKY, the navigator echoes were acquired without additional scan time, which was enabled by exploiting the catalyzation cycles of the SSFP sequence.

References: [1] Kwon et al., MRM 2014; doi: 10.1002/mrm.25452. [2] Liu et al., JMRI 1998;8:903. [3] Ruppert et al., 11th ISMRM, p.208, 2003. [4] Liu et al., MRI 1999;17:689. [5] Shinnar et al., MRM 1994;32:658, [6] Pauly et al., IEEE TMI 1991;10:53.

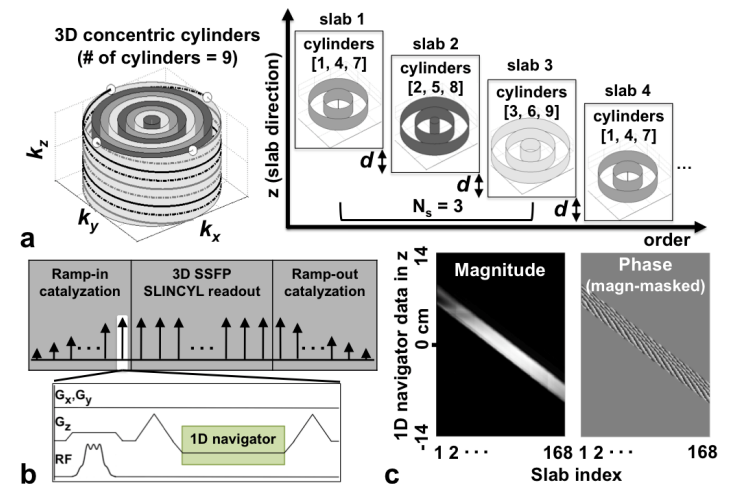


Fig. 1. **a:** Data acquisition scheme of SLINCYL (right). A partial set out of 9 total concentric cylinders (left) is collected at each slab in an interleaved way, which repeats every $N_s = 3$ slabs. **b:** Pulse sequence diagram around the SSFP readout of each slab. A 1D navigator echo is acquired during the ramp-in catalyzation cycles. **c:** 1D navigator data collected as illustrated in (b) for an in vivo scan. Phase offsets due to factors such as RF transmit frequencies and RF excitation profiles are well captured across 168 overlapped thin slabs.

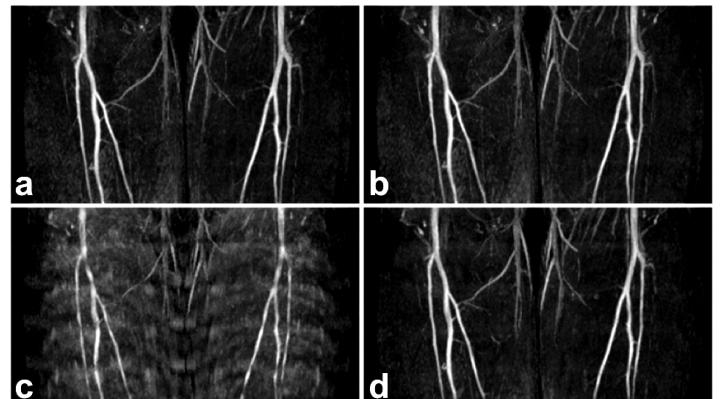


Fig. 2. Targeted coronal MIP images of the calves acquired with LP (top) and NLP (bottom) pulses. **a,c:** With theoretically calculated phase correction. **b,d:** With navigator-based phase correction.